Nanocomposite Gels via in Situ Photoinitiation and Disassembly of TiO₂−Clay Composites with Polymers Applied as UV Protective Films

Chuanan Liao, Qing Wu, Teng Su, Da Zhang, Qingsheng Wu, and Qigang Wang*

Department of Chemistry, Tongji University, Shanghai 200092, P.R. China

Ⓢ *Supporting Information*

ABSTRACT: We report a facile solution polymerized approach to prepare nanocomposite hydrogels. The electrostatic assembly of positive TiO₂ nanoparticles with negative clay nanosheets obtained TiO₂−clay composite particles, which was disassembled by the solution polymerization of *N,N*-dimethylacrylamide and homogeneously interacted with poly(*N,N*-dimethylacrylamide) chain to form nanocomposite hydrogels. The final nanocomposite hydrogels are mechanical tough and transparent, which has the maximum 598.21 KPa compressive strength. The immobilized TiO₂ not only acted as the photo-initiator for radical polymerization but also endowed the nanocomposite gel films good UV protective performance. This strategy can be very useful for preparing nanocomposite hydrogels with different functions.

KEYWORDS: naocomposite hydrogel, UV protection, TiO₂, photopolymerization, electrostatic assembly
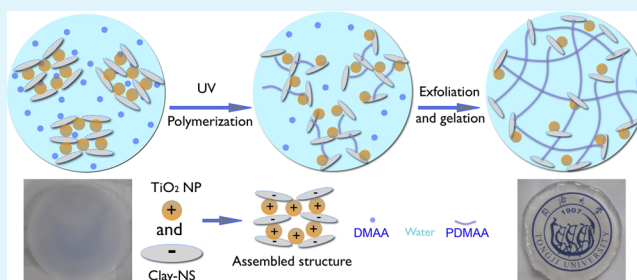
INTRODUCTION

Organic−inorganic nanocomposite, inspired from natural bone and tooth, has attracted increasing attention in recent years because of its wide applications.[1,2] Nanocomposite hydrogels are emerging to be the new star of organic−inorganic hybrid materials because of their water-rich porous structure and excellent performance.[3−5] The dispersion of inorganic components in nanocomposite materials strongly affect the performance of products.[6,7] Among all these inorganic components, clay is one of the most commonly used inorganic components in hydrogels. Clay-based nanocomposite hydrogels have shown ultrahigh mechanical properties due to the multiple noncovalent effects between the monodispersed clay nanosheets and polyacrylamide chains.[8−10] Our group also prepared tough clay nanocomposite hydrogels via the mild photoinitiation of semiconductor nanoparticles.[11] The supramolecular hydrogel formed by mixing sodium polyacrylate dispersed clay with dendritic polymers also demonstrated excellent mechanical property.[12] Other inorganic nanoparticles hybrid polymer hydrogels could not achieve the same strength as that based on clay due to worse dispersed nature and amounts.[13,14]

The in situ preparation of inorganic nanoblocks during hydrogelation can broaden the kinds and forms of nanocomposite hydrogels. As an analogical famous example, the melting intercalation method for the preparation of nylon−clay nanocomposite has been applied in automobile industry.[15−17] The solution intercalation method is another relatively low-cost approach to realize the exfoliation of the layered complex to obtain nanosheets by inserting the large size counter ion in solution phase.[18,19] Here, we combine this solution exfoliation

and the preparation of nanocomposite hydrogel within one experiment process.

RESULTS AND DISCUSSION

Our system consists of four components: TiO₂ nanoparticles (TiO₂-NP), clay nanosheets (clay-NS), *N,N*-dimethylacrylamide (DMAA), and water (Figure 1a). At first, the positive TiO₂ nanoparticles can be electrostatically assembled with the negatively charged clay nanosheets to form the micrometer-sized TiO₂−clay composite (micro-TCC) (Figure 1b). The precursor solution can be simply prepared by the mixing of micro-TCC with the aqueous solution of monomer (Figures 1c and 2a). The monomer molecules would diffuse into the assembled structure of micro-TCC. It is well-known that TiO₂ and other semiconductors are capable of initiating polymerization of monomers under UV irradiation by generating valence-band hole and hydroxyl radical.[11,20,21] Then, the reassembly of the particles was realized by the in situ polymerization of monomer initiated by the TiO₂-NP (Figure 1d). The structure of micro-TCC would be dis-assembled to the dispersed TiO₂-NP and clay-NS in the system. At last, the gels were obtained via the supramolecular crosslinking between the inorganic components with polymer chains (Figures 1e and 2b). For UV protection, TiO₂, a wide band-gap semiconductor with notable photochemical activity, could be a promising candidate due to its high protective properties towards UV light.[22,23] Therefore, our nanocomposite gel films with the
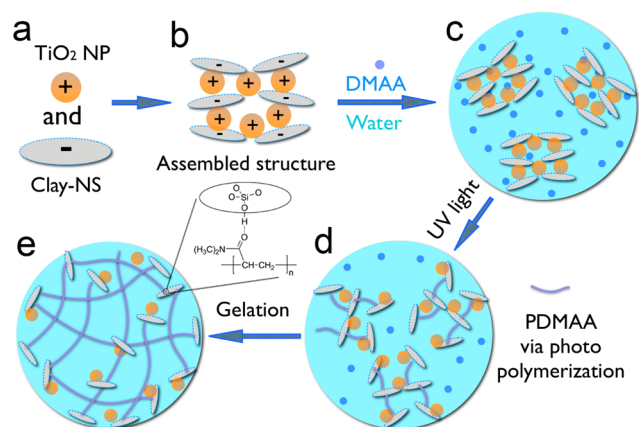
Figure 1. (a) Starting components of TiO_2-NP and clay-NS. (b) Micro-TCC formed by electrostatic assembly. (c) Precursor solution including DMAA (10 wt %) and micro-TCC. (d) Disassembly of micro-TCC by the UV irradiation. (e) Final formation of the TiO_2-based nanocomposite gel under further UV irradiation.
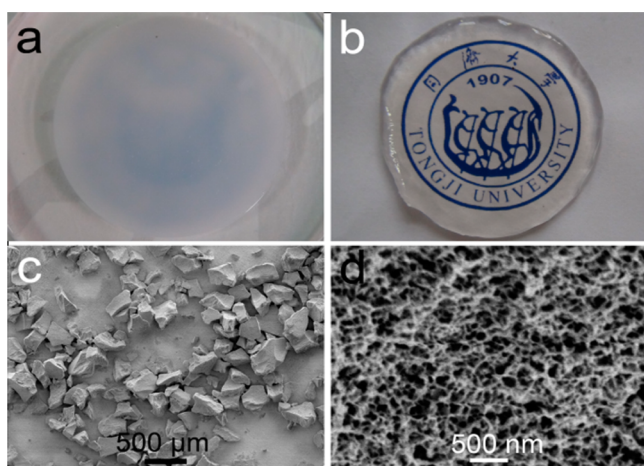

Figure 2. Photos and morphological analysis of precursor and nanocomposite gel. Picture of (a) the turbid precursor solution and (b) the transparent nanocomposite gel. SEM images of (c) the Micro-TCC particles and (d) the TiO_2-based nanocomposite gel.

dispersed TiO_2-NP can be applied in the field of UV protection. The preparation, mechanism and protective performance are shown as follow.

Our approach integrated the solution exfoliation and the gelation together, which can prepare nanocomposite hydrogels by the photoinitiated polymerization of the mixing solution of micro-TCC particles and monomer. The preparation of micro-TCC is very simple. First, 3.0 g clay-NS were dispersed in 600 mL of distilled water to form clean dispersion after 15 minutes stirring (with pH approx. 11). Then, 5 ml solution of positively charged TiO_2 nanoparticles with 10−20 nm size (15 wt %) was added to the previous clay dispersion. At last, 0.5 mL of pure acetic acid was slowly added into the previous mixture to adjust pH to about 5.0, where the precipitation formed immediately. The particles were collected by vacuum filtration of the precipitation. The morphological measurements can provide the solid evidence for the previous preparation and hypothesis.

Scanning electron microscopy (SEM) image shows that the micro-TCC comprised slablike crystal with several ten to several hundred micrometers lateral size and several micrometers thickness (Figure 2c), which indicates the assembly of

TiO_2-NP with CNS. The precipitation of micro-TCC is attributed to the electrostatic interaction of the negatively charged CNS and the positive TiO_2-NP (see Figure S1 in the Supporting Information). The weight ratio of TiO_2-NP to CNS is calculated to be 14.36:85.64 in dried sample of the typical micro-TCC via the ICP-AES measurement. The comparison of their broad angle X-ray diffraction (XRD) also indicates the existence of the original TiO_2-NP and clay-NS in the final micro-TCC (see Figure S2a in the Supporting Information). At the same time, the formation of assembled structure between TiO_2-NP and CNS was confirmed by the existing of a weak diffraction peak at 0.8° in the small-angle X-ray diffraction (see Figures S2b and S3 in the Supporting Information). The value of interlayer space is equal to the addition of about 1 nm thickness of CNS and the approx. 10−20 nm average diameter of TiO_2-NP, which can be calculated from the transmission electron microscopy (TEM) image (see Figure S4a in the Supporting Information).

The preparation of our nanocomposite gels via simple UV polymerization has short polymerization time and mild operation condition. At first, the turbid dispersion of precursor (Figure 2a) was prepared by adding 0.04 g of micro-TCC into the water solution of DMAA (0.2 g in 1.76 mL H_2O) with 15 min vigorous stirring. Then, the transparent TiO_2-based nanocomposite hydrogel (Figure 2b) was gradually formed from the turbid dispersion during 1.5 h UV irradiation (average intensity of 2.0 mW/cm² at 365 nm). The freeze-dried gel exhibits porous network structure with 100−300 nm pore size as shown in SEM image (Figure 2d). When the solid concentration of micro-TCC in hydrogel is larger than 2%, the inorganic components is partly exfoliated to form a translucent even white gel with partial intercalated structures (see Figure S5 in the Supporting Information). TEM image also shows the homogeneous dispersion of TiO_2-NP and CNS within the nanocomposite gel (see Figure S4b in the Supporting Information).

Our method is triggered by the free radical polymerization of DMAA within the micro-TCC. At first, the photogenerated holes around TiO_2 react with the noncovalent adsorbed DMAA to form a surface monomer radical, which initiates the polymerization directly around TiO_2 surfaces.[11] The TiO_2 nanoparticles should be immobilized within the functional hydrogels via noncovalent cross-linking. The EPR spectroscopy of the solution containing micro-TCC and DMPO show four peaks with 1:2:2:1 ratio (Figure 3), confirming hydroxyl radical as another initiating radical in the reaction. Similarly, the EPR spectroscopy of the solution containing micro-TCC and
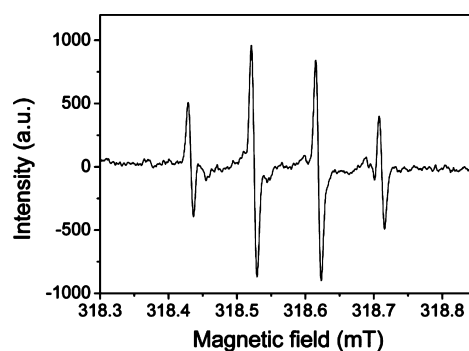

Figure 3. EPR spectrum of the solution of micro-TCC and DMPO under UV irradiation.

DMAA proved the existence of chain propagating radical (see Figure S6 in the Supporting Information). As a result, the UV adsorption of our hydrogel has not obvious change after three swell-drying cycles due to the immobilization of TiO$_2$ nanoparticles (see Figure S7 in the Supporting Information).

The polymerization kinetics can also be characterized by ^{1}H NMR spectroscopy (see Figure S8 in the Supporting Information). The conversion of monomer is higher than 94% after 1 h UV irradiation. At the starting stage, the interlayer space of micro-TCC particles is 11-21 nm according the calculation and SAXD result in Figure S2b in the Supporting Information. The large interlay space of micro-TCC particles will change bigger and bigger along during the photoinitiated polymerization. Their interlay structure will be exfoliated to form the well-dispersed inorganic components. Finally, the formed polymer will cross-link with the inorganic components to form the nanocomposite gels.

The nanocomposite hydrogels exhibit good toughness and elasticity. The compressive strength of these nanocomposite hydrogels is highly relevant to the contents of both components of the gel. Figure 4 shows the comparison of compressive
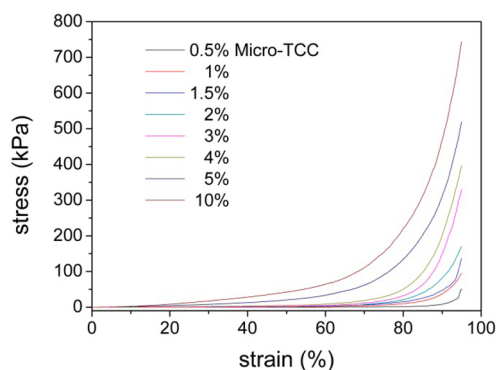

Figure 4. Compressive properties of the TiO$_2$-based nanocomposite hydrogels containing 10% DMAA and different Micro-TCC concentrations.

strength of nanocomposite hydrogels with 0.5−10% Micro-TCC and constant 10% DMAA. The Young's modulus and compressive strength both increase with the increase in micro-TCC content. As shown in Table 1, when the content of micro-TCC increases from 0.5 to 10% with constant 10% DMAA, the Young's modulus increases from 0.47 to 36.99 kPa, whereas the

compressive strength at 95% compression increases from 50.22 to 598.21 kPa. The use of clay as inorganic cross-linker can significantly enhance the mechanical performance of hydrogel (see Figure S9 in the Supporting Information). At the same time, the existing of TiO$_2$ nanoparticles can exactly enhance the mechanical property (see Figure S10 in the Supporting Information). Therefore, the mechanical performance should be ascribed to the cooperative reinforcement of both TiO$_2$-NP and clay-NS to the gel.

The inorganic components are the main reinforcement fillers and crosslinking points of our nanocomposite hydrogel, which contribute to the mechanical properties. At the same time, the compressive strength is slightly enhanced with the increase in DMAA content. The Young's modulus only increases from 1.66 to 2.62 kPa and the compressive strength at 95% compression increases from 88.45 to 201.63 kPa, when the content of DMAA increases from 1 to 10% with constant micro-TCC content (Table 1 and Figure S11 in the Supporting Information). The increase in monomer content can enhance the density of polymer chains and the mechanical strength of the resulted gels. The tensile properties of our gels with 10% DMAA and 2% Micro-TCC are listed in Figure S12 in the Supporting Information. The tensile strength and elongation are 63.75 kPa and 21.2 times, respectively. On the basis of the tensile curves, we can calculate the index of toughness. The index of toughness is the total work required for the fracture of a unit volume of a material, which was calculated by the area under the tensile stress—strain curves.[24,25] As shown in Table 1, the value of toughness has the similar trends with compressive strength.

The TiO$_2$-based nanocomposite gels can be prepared in various forms, i.e., bulk hydrogel and film. This gelated approach with viscous suspension is also a new exploration to prepare nanocomposite gel in organic-water hybrid solvent. Acetone, acetonitrile and dimethylformamide were employed in our system to prepare the nanocomposite gel with 1:1 volume ratio of water to solvent. The optical images and mechanical properties of the gels prepared with mixed solvents were tested and shown (see Figure S13 in the Supporting Information). It is found that the nanocomposite hydrogel has higher compressive strength than all the gels prepared with mixed solvents. This result demonstrates that our approach can be easily applied in miscible solvents, where the nanocomposite gels cannot be obtained by direct cross-linking of inorganic nanoparticles and polymer.

Table 1. Mechanical Properties of Nanocomposite Gels

DMAA/micro-TCC	appearance	Young's modulus (kPa)[a]	compressive strength (kPa)	toughness (MJ/m^3)
10/0.5	transparent	0.47 ± 0.02	50.22 ± 2.51	[b]
10/1	transparent	0.50 ± 0.02	96.39 ± 4.82	[b]
10/1.5	translucent	1.65 ± 0.08	125.20 ± 6.26	0.006 ± 0.001
10/2	translucent	2.62 ± 0.13	201.63 ± 10.08	0.65 ± 0.03
1/2	translucent	1.66 ± 0.08	88.45 ± 4.42	[b]
3/2	translucent	2.01 ± 0.10	147.35 ± 7.37	[b]
5/2	translucent	2.15 ± 0.11	164.06 ± 8.20	0.25 ± 0.01
7/2	translucent	2.22 ± 0.11	182.07 ± 9.10	0.40 ± 0.02
10/3	translucent	5.13 ± 0.26	282.98 ± 14.15	1.20 ± 0.06
10/4	translucent	7.63 ± 0.38	353.56 ± 17.68	1.91 ± 0.10
10/5	white	11.11 ± 0.56	403.21 ± 20.16	3.15 ± 0.16
10/10	white	36.99 ± 1.85	598.21 ± 29.91	3.91 ± 0.20

[a]The range of strain region for Young's modulus is 5−15%. [b]Undetectable.

The tough nanocomposite gels are new candidates for the application of UV protective application due to the homogenously dispersed TiO_2-NP within the transparent platform. Figure 5a shows the UV−vis spectra of the
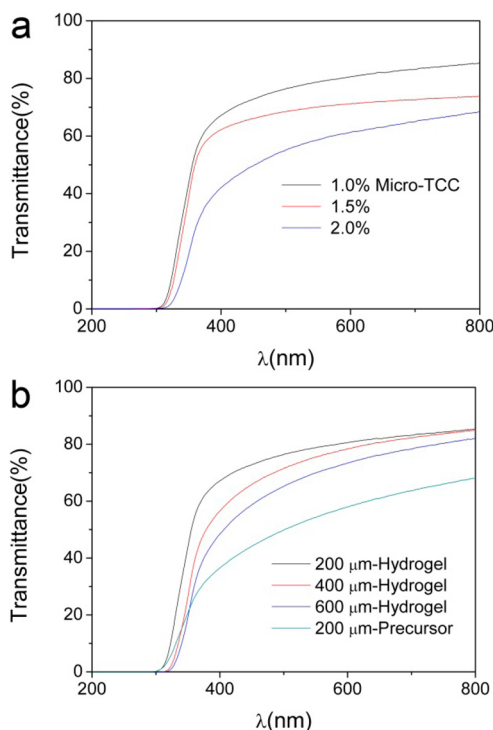

Figure 5. UV−vis transmittance spectra of the TiO_2-based nanocomposite hydrogel films with (a) the same thickness of 200 μm containing 10% DMAA and different micro-TCC content, (b) with different thickness.

nanocomposite hydrogels film (about 200 μm) with different contents of micro-TCC. The transparency of the film decreases in the visible-light region (400-800 nm) with the increased content of micro-TCC. For example, the transmittance of the film at 600 nm decreases to 80.6, 71.2, and 61.3% as the content of micro-TCC increases to 1.0, 1.5, and 2.0%, respectively, whereas in the UV light region (200−400 nm), the transmittance of the films all decreases sharply to zero. The gel film with the higher micro-TCC content can achieve zero transmittance at higher wavelength. In a word, the UV shielding property of the film is enhanced with the increase in micro-TCC content. At the same time, the transparency at visible region decreases with the increasing content of the inorganic components.

It is well-known that the dispersed TiO_2-NPs in our gel films are the main reason for the UV screening ability. The optical adsorption edge of TiO_2 was measured to be 327 nm (see Figure S14 in the Supporting Information), showing a big blue shift to that of the bulk anatase TiO_2 (388 nm, 3.2 eV).[26,27] This is similar to other semiconductor nanoparticles systems, which may result from the quantum size effects of the nanoparticles with the sharply decreased size.[28,29] Figure 5b shows the UV−vis spectra of the nanocomposite film with different thickness of 200, 400, and 600 μm. The transparency of the films in the range of visible region decreases along with the increasing thickness. In the UV region, the thicker the film, the more UV light absorbed. The thicker film should contain more TiO_2-NPs, which contributes to the shielding of both the

UV light and the visible light. The hybrid gel film containing only TiO_2 and organic cross-linkers showed the almost same screening effect during UV range (see Figure S15 in the Supporting Information). The higher transmission at visible-light range of our gel relative to gel with only TiO_2 should be ascribed to the enhanced dispersion of TiO_2 nanoparticles. The hybrid gel film with single clay-based gel formed by organic photo-initiator further confirm the clay and poly(N,N-dimethylacrylamide) (PDMAA) has not the obvious screening effect. Therefore, clay is necessary to achieve an elastic gel film with excellent UV screening ability.

In addition, as is shown when comparing the UV−vis spectra of the precursor solution with the nanocomposite hydrogel at the same thickness of 200 μm, the transmittance raises evidently after the formation of the hydrogel, indicating that the inorganic components distribute more homogeneously in the hydrogel than in the precursor solution. The refractive index of our gel film with 231 nm thickness is about 1.37 at 500 nm wavelength. To evaluate the ultraviolet radiation protective properties, we have determined ultraviolet protection factors (UPF) for the gels referring to the standard of textiles. The ultraviolet protection factor is 91.3 and 10.8 at the UVB and whole UV range, respectively.

CONCLUSIONS

In this paper, we describe the preparation of UV-screening nanocomposite gels by photo-initiated polymerization. The positive TiO_2 NP were found to form the composite with negative CNS via electrostatic assembly. The immobilized TiO_2 remain the function as the initiators under UV irradiation. Along with the photo polymerization, TiO_2-clay composite particles was dis-assembled and homogeneously dispersed with PDMAA chain to form nanocomposite hydrogels. The TiO_2-based nanocomposite gels in various forms can be prepared for different application. As a demonstration, the TiO_2-based nanocomposite gel films show good UV protective performance.

ASSOCIATED CONTENT

Ⓢ Supporting Information

Experimental details, images and XRD, TEM analyses for the formation of the Micro-TCC, EPR, NMR characterization of the gelling process, mechanical properties of other hydrogels, and UV absorption edge of the TiO_2-NP. This material is available free of charge via the Internet at http://pubs.acs.org/.

AUTHOR INFORMATION

Corresponding Author
*E-mail: wangqg66@tongji.edu.cn.
Notes
The authors declare no competing financial interest.

ACKNOWLEDGMENTS

ABBREVIATIONS

TiO_2−NP, TiO_2 nanoparticles

clay-NS, clay nanosheets
micro-TCC, micrometer-sized TiO_2−clay composite
DMAA, *N,N*-dimethylacrylamide
PDMAA, poly(*N,N*-dimethylacrylamide)

■ REFERENCES

(1) Fox, J.; Wie, J. J.; Greenland, B. W.; Burattini, S.; Hayes, W.; Colquhoun, H. M.; Mackay, M. E.; Rowan, S. J. *J. Am. Chem. Soc.* **2012**, *134*, 5362−5368.

(2) Tang, L.; Weder, C. *ACS Appl. Mater. Interfaces* **2010**, *2*, 1073−1080.

(3) Liu, J.; Chen, C.; He, C.; Zhao, J.; Yang, X.; Wang, H. *ACS Nano* **2012**, *6*, 8194−8202.

(4) Yang, J.; Han, C. -R; Duan, J. -F.; Xu, F.; Sun, R. -C. *ACS Appl. Mater. Interfaces* **2013**, *5*, 3199−3207.

(5) Wang, H.; Shi, Y.; Wang, L.; Yang, Z. *Chem. Soc. Rev.* **2013**, *42*, 891−901.

(6) Paul, D.; Robeson, L. *Polymer* **2008**, *49*, 3187−3204.

(7) Potts, J. R.; Dreyer, D. R.; Bielawski, C. W.; Ruoff, R. S. *Polymer* **2011**, *52*, 5−25.

(8) Haraguchi, K.; Takehisa, T. *Adv. Mater.* **2002**, *14*, 1120−1124.

(9) Chang, C. -W.; van Spreeuwel, A.; Zhang, C.; Varghese, S. *Soft Matter* **2010**, *6*, 5157−5164.

(10) Haraguchi, K.; Li, H. J.; Matsuda, K.; Takehisa, T.; Elliott, E. *Macromolecules* **2005**, *38*, 3482−3490.

(11) Zhang, D.; Yang, J.; Bao, S.; Wu, Q.; Wang, Q. *Sci. Rep.* **2013**, *3*, 1399.

(12) Wang, Q.; Mynar, J.L.; Yoshida, M.; Lee, E.; Lee, M.; Okuro, K.; Kinbara, K.; Aida, T. *Nature* **2010**, *463*, 339−343.

(13) Zou, H.; Wu, S.; Shen, J. *Chem. Rev.* **2008**, *108*, 3893−3957.

(14) Zhu, C. H.; Hai, Z. B.; Cui, C. H.; Li, H. H.; Chen, J. F.; Yu, S. H. *Small* **2012**, *8*, 930−936.

(15) Kojima, Y.; Usuki, A.; Kawasumi, M.; Okada, A.; Fukushima, Y.; Kurauchi, T.; Kamigaito, O. *J. Mater. Res.* **1993**, *8*, 1185−1189.

(16) Usuki, A.; Kojima, Y.; Kawasumi, M.; Okada, A.; Fukushima, Y.; Kurauchi, T.; Kamigaito, O. *J. Mater. Res.* **1993**, *8*, 1179−1184.

(17) Cho, J.; Paul, D. *Polymer* **2001**, *42*, 1083−1094.

(18) Wang, Q.; Gao, Q.; Shi, J. *J. Am. Chem. Soc.* **2004**, *126*, 14346−14347.

(19) Liu, Z.; Ma, R.; Osada, M.; Iyi, N.; Ebina, Y.; Takada, K.; Sasaki, T. *J. Am. Chem. Soc.* **2006**, *128*, 4872−4880.

(20) Ni, X.; Ye, J.; Dong, C. *J. Photochem. Photobiol., A* **2006**, *181*, 19−27.

(21) Nakashima, T.; Sakashita, M.; Nonoguchi, Y.; Kawai, T. *Macromolecules* **2007**, *40*, 6540−6544.

(22) Ren, Y.; Chen, M.; Zhang, Y.; Wu, L. *Langmuir* **2010**, *26*, 11391−11396.

(23) Xiao, J.; Chen, W.; Wang, F.; Du, J. *Macromolecules* **2013**, *46*, 375−383.

(24) Nakajima, T.; Sato, H.; Zhao, Y.; Kawahara, S.; Kurokawa, T.; Sugahara, K.; Gong, J. P. *Adv. Funct. Mater.* **2012**, *22*, 4426−4432.

(25) Naficy, S.; Brown, H. R.; Razal, J. M.; Spinks, G. M.; Whitten, P. G. *Aust. J. Chem.* **2011**, *64*, 1007−1025.

(26) Tang, H.; Berger, H.; Schmid, P.; Levy, F.; Burri, G. *Solid State Commun.* **1993**, *87*, 847−850.

(27) Long, R.; English, N. J. *J. Phys. Chem. C* **2010**, *114*, 11984−11990.

(28) Frame, F. A.; Osterloh, F. E. . *J. Phys. Chem. C* **2010**, *114*, 10628−10633.

(29) Waller, M. R.; Townsend, T. K.; Zhao, J.; Sabio, E. M.; Chamousis, R. L.; Browning, N. D.; Osterloh, F. E. *Chem. Mater.* **2012**, *24*, 698−704.

■ NOTE ADDED AFTER ASAP PUBLICATION

This paper was published on the Web on January 21, 2014, with incorrect units in the text describing Figure 2d. The corrected version was reposted on January 23, 2014.